

# NUMERICAL INVESTIGATION OF ISLAND EFFECTS ON DEPTH AVERAGED FLUCTUATING FLOW IN THE PERSIAN GULF

Saeed-Reza Sabbagh-Yazdi\* and Mohammad Zounemat-Kermani

Department of Civil Engineering, K. N. Toosi University of Technology  
Valiasr St., Tehran, Iran

SYazdi@kntu.ac.ir - zounemat@computermail.net

\*Corresponding Author

(Received: September 29, 2005 – Accepted in Revised Form: March 18, 2007)

**Abstract** In the present paper simulation of tidal currents on three-dimensional geometry of the Persian Gulf is performed by the solution of the depth averaged hydrodynamics equations. The numerical solution was applied on two types of discretized simulation domain (Persian Gulf); with and without major islands. The hydrodynamic model utilized in this work is formed by equations of continuity and motion in two-dimensional horizontal plane. The effects evaporation and rainfall are considered in the source term of the continuity equation. The effects of bed slopes in x and y directions are considered in the partial differential terms representing the variation of hydrostatic pressure and the effects of bed friction, as well as the Coriolis effects are considered in algebraic terms of two equations of motion. The unstructured finite volume method is applied for solving the governing equations on overlapping control volumes formed by triangular cells. Using unstructured triangular meshes provides modeling of the geometrically complex flow domains, such as the Persian Gulf region. The results of the developed model for fluctuating flow on the variable bed elevation are compared with an available analytical solution of flow in a quadrant variable bed slope and Parshall flume. The accuracy of the finite volume flow solver is assessed by comparison between numerical results and the analytical solution and experimental measurements reported in the literature. The performance of the computer model to simulate tidal flow in the Persian Gulf domain is examined by imposing tidal fluctuations to the main flow boundary during a limited period of time and comparison of the computed results in an arbitrary location with available data from admiralty tide tables. Finally, a comparison was made between the model results of the two types of discretized simulation domain.

**Keywords** Tidal Flow, Persian Gulf, Unstructured Finite Volumes

**چکیده** در مقاله حاضر نتایج شبیه سازی جریانات جزر و مدی بر روی هندسه سه بعدی خلیج فارس با حل معادلات هیدرودینامیکی جریان میانگین عمقی ارائه گردیده است. مدل هیدرودینامیکی مورد استفاده برای این کار از معادله حرکت در صفحه افق تشکیل شده است. تاثیر تبخیر و بارندگی در یک عبارت جبری در معادله پیوستگی لحاظ شده است. تاثیرات استهلاک ناشی از زبری بستر جریان و نیروهای ناشی از گردش زمین در عبارات جبری معادلات حرکت و تاثیر شیب بستر در عبارت مشتق پاره ای نمایانگر تغییرات فشار هیدرواستاتیک معادلات مذکور، منظور شده است. برای حل عددی معادلات شبکه بی ساختار احجام محدود تشکیل شده از سلولهای مثلثی بکار برده شده است. استفاده از این نوع شبکه مدلسازی محیط های آبی با هندسه پیچیده همچون خلیج فارس را امکان پذیر می سازد. برای صحت سنجی تحلیلگر احجام محدود جریان، نتایج مدلسازی جریان دو بعدی ناشی از نوسانات سطح آب در حوضه ای به شکل یک چهارم حلقه با شیب متغیر بستر با حل تحلیلی مسئله مورد مقایسه قرار گرفته است. همچنین نتایج مدلسازی جریان در یک پارشال فلوم با اندازه گیری های گزارش شده در مقالات محققین دیگر مقایسه شده اند. در نهایت کارائی مدل تدوین شده با شبیه سازی جریان های دریائی در خلیج فارس که عمدتاً از نوسانات جزر و مدی در تنگه هرمز ناشی می شوند، مورد آزمون قرار گرفته است. نتایج مدلسازی جریانات جزر و مدی در خلیج فارس در بندر بوشهر برای یک دوره زمانی محدود با نتایج اطلاعات حاصل از آنالیز هارمونیک جداول نیروی دریائی انگلستان مقایسه شده است.

## 1. INTRODUCTION

Industrial growth has resulted significant increase

in oil consumption. The Persian Gulf region is one of the major resources which support the crude oil requirements of the world. A significant amount of

oil is spilled into the sea from offshore drilling and operational discharges of ships as well as accidental tanker collisions and groundings. Since the Persian Gulf is a closed basin and is connected to the Indian Ocean via the HORMOZ Strait, the vulnerable marine environment of this region is an important reason for studying the Persian Gulf water currents. Therefore, due to on-shore and off-shore activities of Iran and Arabian countries for oil production and shipping, the hydrodynamics of the Persian Gulf region has become of great importance.

Recent advances in production of high performance computers and rapid development of efficient numerical modeling techniques have paved the way for application of efficient and accurate numerical algorithm.

Although, three-dimensional flow solvers are accurate, they are computationally expensive due to required number of elements and numerical techniques for modeling fluctuation of water free surface.

Two-dimensional depth averaged models are well established models where the vertical velocity components are not significant in comparison with horizontal components.

Vast areas of the Persian Gulf (with 1000 km length, 340 km maximum width and less than 0.1 km maximum depth) is shallow and only one third of the region has more than 0.04 km depth. Therefore, two-dimensional tidal currents in the Persian Gulf may be modeled using depth averaged hydrodynamic model.

Some of the numerical models of the Persian Gulf reported in the literature have used two-dimensional depth averaged hydrodynamic equations in Cartesian coordinates system [1,2]. In order to get more accurate results, in some modeling efforts the two-dimensional depth average equations are transformed into spherical system [3,4]. Most of these models use finite difference method for solving the utilized hydrodynamic equations.

A numerical model is not able to simulate the real world flow pattern unless the geometrical characteristics of flow domain (i.e. irregularities of coasts and bed surface topography) are modeled precisely. Thus, the numerical flow solver should handle the geometrical complexities of the bed and boundaries of the flow domain. Therefore, in the

present work, to overcome the problem, NASIR (Numerical Analyzer for Scientific and Industrial Requirements) hydrodynamic solver model was used, which utilizes the depth averaged hydrodynamic equations on unstructured finite volumes. The flow solver is tested for modeling a fluctuating two-dimensional flow on a bed with a variable slope, and the ability at flow solver to handle flow with transient regimes is by solution of flow in a Parshall flume. Then, the model is applied to simulate tidal currents in the Persian Gulf.

## 2. GOVERNING EQUATIONS

The vector form of depth-integrated continuity and momentum equations of free surface water flow are:

$$\frac{\partial}{\partial t}(h) + \frac{\partial}{\partial x_j}(hu_j) = Q_z \quad (j=1,2) \quad (1)$$

$$\frac{\partial}{\partial t}(hu_i) + \frac{\partial}{\partial x_j}(hu_i u_j) + \frac{1}{2}gh \frac{\partial}{\partial x_i}(\eta) =$$

$$f_{ci} - \frac{\tau_{bi}}{\rho_w} + \frac{\tau_{si}}{\rho_w} + \frac{\partial}{\partial x_j}, \quad (j=1,2) \quad (2)$$

Using the above equations, the currents in the Persian Gulf are computed considering  $Q_z$  the rainfall-evaporation from unit area of water surface and bed slopes,  $\eta = h + z_b$ , global bed friction stresses  $\tau_{bi} = \rho_w C_f u_i |U|$

( $C_f = g n^2 / h^{0.33}$  using  $n$  manning coefficient), global wind stresses on water surface

$\tau_{si} = \rho_{air} C_w v_{wi} |V_{wind 10m}|$  (with  $C_w = 0.001$ ),

Coriolis forces due to earth rotation  $f_{cx} = -hu_y \omega \sin \phi$  and  $f_{cy} = +hu_x \omega \sin \phi$  using  $\omega$  earth angular velocity and  $\phi$  the geographical latitude of the point [5].

The trace-free turbulent stress

$\tau_{ij} = hv_{ht} \left( \frac{\partial u_i}{\partial x_j} + \frac{\partial u_j}{\partial x_i} \right)$  can be computed after

determining the value of the horizontal eddy viscosity parameter by application of the widely

used parabolic mixing length formulation  $v_{ht} = \alpha h U^*$ . In this formulation the bed friction velocity is defined as  $U^* = [\tau_{ib} / \rho_w]^{0.5}$  and the empirical coefficient  $\alpha$  is advised between 0.1 and 1.0 [6].

### 3. NUMERICAL SOLUTION

Considering the governing equations in form of an advection-diffusion type equation,  $W$  represents the conserved variables using  $h$  flow depth,  $u$  and  $v$  the horizontal components of velocity  $G^c$  and  $F^c$  are vectors of convective fluxes, while,  $G^d$  and  $F^d$  are vectors of diffusive fluxes of  $W$  in  $x$  and  $y$  directions, respectively. The vector  $S$  contains the sources and sinks of the governing equations covering all algebraic terms.

$$\frac{\partial W}{\partial t} + \left( \frac{\partial F^c}{\partial x} + \frac{\partial G^c}{\partial y} \right) = \left( \frac{\partial F^d}{\partial x} + \frac{\partial G^d}{\partial y} \right) + S \quad (3)$$

The above equation is discretized by application of the cell vertex (overlapping) scheme of the finite volume method. This method ends up with the following formulation [7]:

$$W_i^{t+\Delta t} = W_i^t - \frac{\Delta t}{\Omega_i} \left[ \sum_{k=1}^{N_{sides}} [(\bar{F}^c \Delta y - \bar{G}^c \Delta x) - (F^d \Delta y - G^d \Delta x)]_k \right] + S_i^t \Delta t \quad (4)$$

Where  $W_i$  represents conserved variables at the center of control volume  $\Omega_i$ .  $\bar{F}^c$  and  $\bar{G}^c$  are the mean values of convective fluxes on the control volume boundary sides. The diffusive fluxes  $F^d$  and  $G^d$  are computed using a discrete formula of contour integral around the centre of the control volume boundary sides (using an auxiliary control volume).

$$\text{The residual term, } R(W_i) = \sum_{k=1}^{N_{sides}} [(\bar{F}^c \Delta y - \bar{G}^c \Delta x) - (F^d \Delta y - G^d \Delta x)]_k,$$

consists of convective and diffusive parts. In smooth parts of the flow domain, where there are no strong gradient of flow parameters, the convective part of the residual term is dominated. Since, in the explicit computation of convective dominated flow there is no mechanism to damp out the numerical oscillations, it is necessary to apply numerical techniques to overcome instabilities with minimum accuracy degradation. In present work, the artificial dissipation terms suitable for the unstructured meshes are used to stabilize the numerical solution procedure. In order to damp the unwanted numerical oscillations, a fourth order artificial dissipation term,

$D(W_i) = \varepsilon \sum_{j=1}^{N_{edges}} \lambda_{ij} (\nabla^2 W_j - \nabla^2 W_i)$  is added to above algebraic formula in which  $\lambda_{ij}$  is a scaling factor and is computed using the maximum value of the spectral radii of every edge connected to node  $i$  ( $1/256 \leq \varepsilon \leq 3/256$ ). Here, the laplacian operator at every node  $i$ ,  $\nabla^2 W_i = \sum_{j=1}^{N_{edges}} (W_j - W_i)$ , is computed using the variables  $W$  at two end nodes of edges (meeting node  $i$ ). The revised formula, which preserves the accuracy of the numerical solution, is written in the following, form

$$W_i^{t+\Delta t} = W_i^t - \frac{\Delta t}{\Omega_i} \{R(W_i^t) - D(W_i^t)\} + S_i^t \Delta t \quad (5)$$

$\Delta t$  is the minimum time step of the domain (proportional to the minimum mesh spacing). In present study, a three-stage Runge-Kutta scheme, which damps high frequency errors, is used for stabilizing the explicit time stepping process [8].

In the above equation, the quantities  $W$  at each node are modified at every time step by adding a residual term which is computed using the quantities  $W$  at the edges of the control volume  $\Omega_i$ . Hence, the edges are referred to all over the computation procedure. Therefore, it would be convenient to use the edge-base data structure for definition of unstructured meshes. Using the edge-base computational algorithm reduces the number of addressing to the memory and provides up to 50 % saving in computational CPU time consumption. Hence, the edge-base algorithm and data structure improves the efficiency shortcoming of the

unstructured mesh data processing.

#### 4. BOUNDARY CONDITIONS

Two types of boundary conditions are applied in this work; flow and solid wall boundary conditions.

The tidal flow boundary condition is considered by imposing water level surface fluctuations in the HORMOZ Strait. In this case, the velocity components in the HORMOZ Strait are extrapolated from the computational domain. The fluctuations of water surface elevation are derived from tidal predictions at Didamar Island, which are obtained through the application of the calibrated constants of the harmonic analysis for any arbitrary period of time [9].

The river inflow is imposed whenever the inside domain water surface level is less than the water level at the flow boundary. The monthly inflow rate of the Arvand River, [10] is suitable to apply for the computation of inflow velocity. In such a case, water surface elevation at the river boundary has to be extrapolated from the computational domain. Otherwise, all the flow parameters have to be extrapolated.

The dry parts at coastal zone boundaries are the flow domain limits. At these boundaries the component of the normal velocities are set to zero. Therefore tangential computed velocities are kept using free slip condition at wall boundaries. Although small water depths in coastal zones give rise to the global bed shear stresses and reduce the computed velocities, tangential velocity reduction may be used to model the effect of wall boundaries.

In shallow coastal water bodies like an embayment, estuaries, lagoons and such, experiencing tidal oscillations of the free surface, the extent of areas subjected to alternating wet and drying (the so-called tidal flats) may be of the same order of magnitude as constantly submerged areas [11]. However, in present work the average size of grid spacing (5km) is much larger than the maximum tidal oscillations (5m). Hence, the extension of tidal flats is not considerable, and therefore, no wet and drying technique is applied in this work.

#### 5. MODEL VERIFICATION

At this part, firstly the hydrodynamic model is examined for fluctuating flow on a test case with variable bed elevations and the numerical results are compared with available analytical solution. Secondly, numerical solution of flow in a Parshall Flume is chosen, in order to investigate the ability of the model to solve the cases with inverse slopes and irregularities in boundaries as well as the trans-critical flow regime.

##### 5.1. Transient Flow In A Quadrant With Bed Slope

In this section, first the hydrodynamic model is examined for fluctuating flow on the variable bed slope and the numerical results are compared with available analytical solution.

The quadrant frictionless channel with a parabolic bed test is recommended to evaluate the performance of tidal numerical models [12]. The geometry of physical domain is the quadrant with an internal radius  $r_1 = 60960$  m, external radius  $r_2 = 152400$  m and bed depth from water mean level  $h = 2.5 \times 10^{12}/r^2$ . The imposed boundary conditions are as follow:

$$\begin{aligned} \frac{\partial \xi}{\partial r} &= 0 & r &= r_1 \\ \xi(r_2, \theta, t) &= \text{Re}[\xi_0(\theta)e^{i\omega t}] & r &= r_2 \\ \frac{\partial \xi}{\partial \theta} &= 0 & \theta &= 0, \pi/2 \end{aligned} \quad (6)$$

Where the parameters are defined as;  $\theta$ : Angle in polar coordinate,  $t$ : time,  $\xi$ : water elevation above mean water level,  $\xi_0$ : tide amplitude,  $\omega$ : angular frequency of tidal function.

The analytical solution of  $\xi$  is given as [12]:

$$\xi(r, t) = \text{Re} \left\{ \xi_0 \frac{\cos \left[ \frac{\beta}{2} (r^2 - r_1^2) \right]}{\cos \left[ \frac{\beta}{2} (r_2^2 - r_1^2) \right]} \cdot e^{i\omega t} \right\}$$

$$\beta^2 = (\omega^2 - i\omega\tau) / gH_0 \quad (7)$$

Here the parameters are;  $g$ : acceleration due to

gravity,  $H_0$ : a real and constant number ( $h = H_0 r^{-2}$ ),  $\tau$ : bed friction constant. However, in order to investigate the effects of the variable bed elevation on tidal flow, the case in the present paper is considered with negligible bed friction.

The flow domain is geometrically modeled in two stages. In the first stage, the horizontal geometry of the problem is modeled by defining four boundary curves. Then, the flow domain is discretized using an unstructured mesh, generated by Deluaney Triangulation Technique, [13].

In order to perform numerical simulations, the domain was discretized with a triangular unstructured mesh which contains 1083 nodes and 1989 cells and then the bed elevations are implemented to nodal points of the mesh.

In the second stage, for converting the two-dimensional mesh into a three dimensional surface, the bed elevation of the flow domain is digitized at a number of points along some contour lines. Then, the bed elevation is set for every node of the mesh by interpolation of the elevations of surrounding digitized points. Therefore, the two dimensional mesh is converted to a three dimensional bed surface of the flow domain see Figure 1.

By imposing tidal (sinusoidal) waves with amplitude, of 0.3048m and period of 12.4hr at outer arc (flow boundary), the flow patterns are computed. The results of the hydrodynamic model and analytical solution are compared for two times see Figure 2. As shown in this figure, the results present good agreement with the analytical solution for the most parts of the flow domain.

**5.2. Parshall Flume** Numerical solution of flow in a Parshall Flume is chosen as a test case to evaluate the model performance in simulating flow in a channel with variable bed slope and width. Rectangular sections and smooth bed surfaces are reported for the selected channel with available experimental measurements [14].

The unstructured triangular adaptively refined mesh utilized for the solution contains 1274 nodes, and 3323 edges. Super-critical free surface flow over the entire channel length is assumed as the initial conditions. Sub and super critical boundary conditions are respectively considered at upstream and downstream of the flume. Hence, unit width discharge is imposed at upstream, while, the upstream flow depth and all flow variables at down

stream are extrapolated from inside of flow domain. In this case, the flow depth is imposed at none of the flow boundaries. Therefore, the computed water surface along the entire channel length is formed from the critical depth, which occurs at the position where flow regime changes [15].

As shown in Figure 3b, sub-critical flow is formed at the right straight reach, while the flow regime is transformed into super-critical at the left straight reach. However at the left straight reach, some shock waves are formed due to sudden changes of the walls and bed slopes. Figure 4 shows the comparison between experimental measurements of the water surface and model results along the central axis of the flume [14]. The computed results present good agreement with measured data at most parts of the channel.

## 6. MODEL APPLICATION

Here, the numerical simulation of currents in the Persian Gulf is presented after evaluation of the accuracy of the developed hydrodynamic model. The performance of the computer model to simulate tidal flow in the Persian Gulf domain is examined by imposing tidal fluctuations to the main flow boundary during a limited period of time.

The flow domain is modeled in two stages. In the first stage, horizontal geometry of the problem is modeled by definition of coastal boundaries. Then, the flow domain is discretized using unstructured mesh generated by Deluaney Triangulation Technique, [13]. In this paper, the effect of considering 8 major islands on flow patterns in the Persian Gulf is investigated. The Persian Gulf simulation domain considering major islands contains 7288 nodes, 13532 elements, and 20828 edges see Figure 5a, while the computational mesh without islands contains 1618 nodes, 2905 elements, and 4522 edges see Figure 5b.

In the second stage, for converting the two dimensional mesh into a three dimensional surface, the bed elevation of the flow domain is digitized at a number of points along contour lines. Then, the bed elevation is set for mesh nails by interpolation of the elevations of surrounding digitized points.

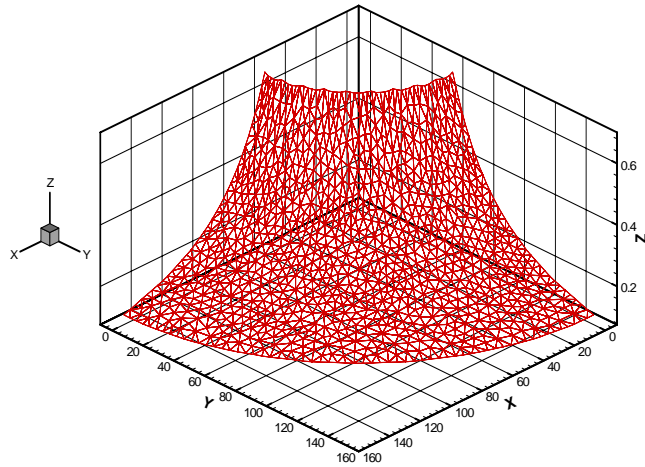


Figure 1. Mesh and geometry of quadrant channel; (a) horizontal plan, (b) 3D view.

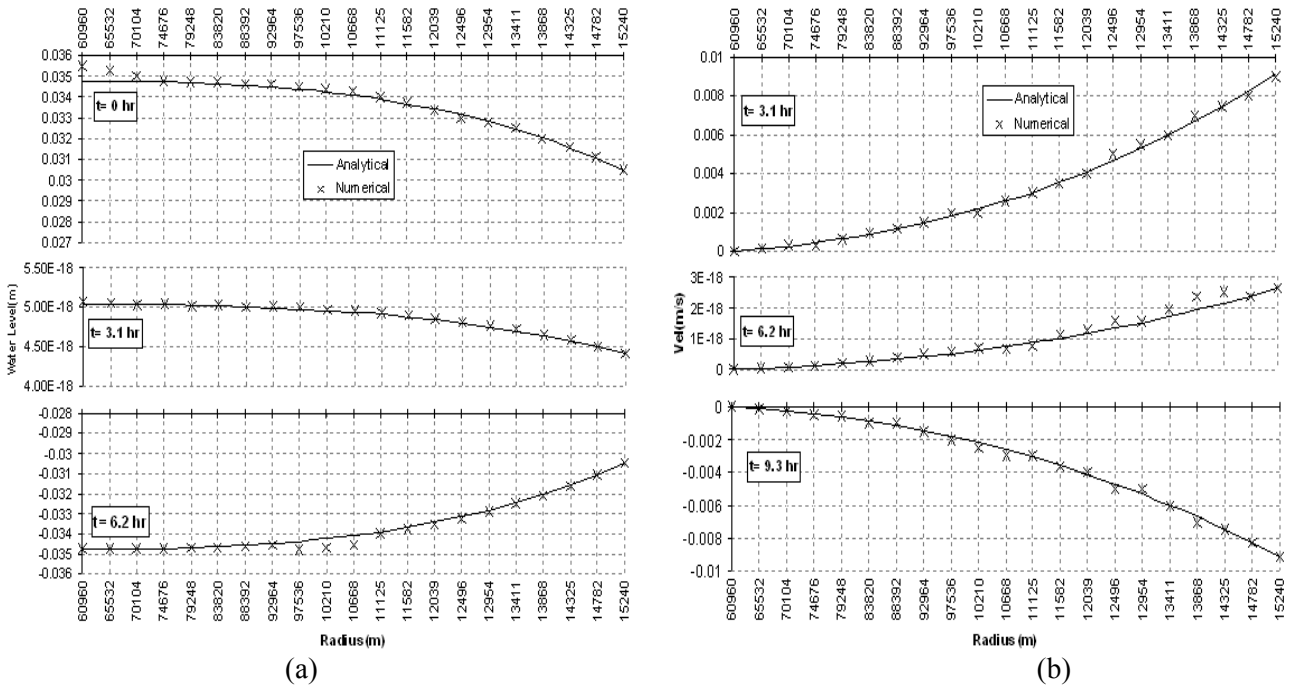


Figure 2. Comparison between numerical results and analytical solution; (a)  $t = 0, 3.1$  and  $6.2$  hours, (b)  $t = 3.1, 6.2$  and  $9.3$  hours.

Therefore, the two dimensional mesh is converted to a three dimensional bed surface of the flow domain.

### 6.1. Modeling Results

The described hydrodynamic model is used to compute flow

patterns in Persian Gulf due to tidal fluctuations at east boundary, river inflow at west coast, evaporation from water surface, Coriolis effect, friction and irregularities of coasts and bed (using unstructured three dimensional surface mesh). In order to verify the quality of the results, the tidal

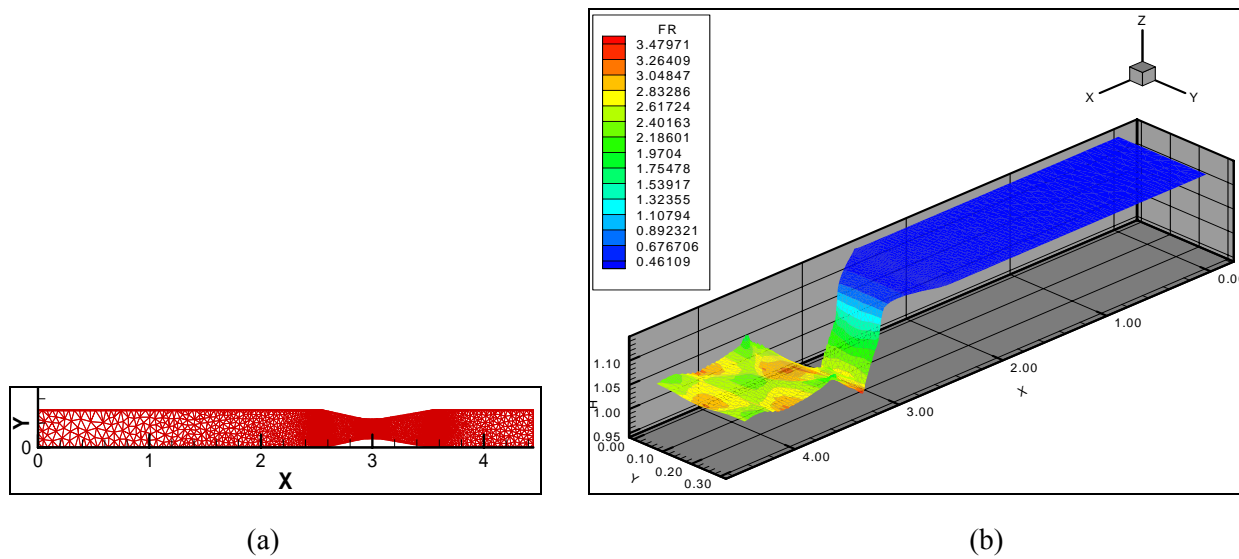


**Figure 3.** (a) Two-dimensional discrete geometrical mode, (b) computed Froude number at the 3-D entire channel.

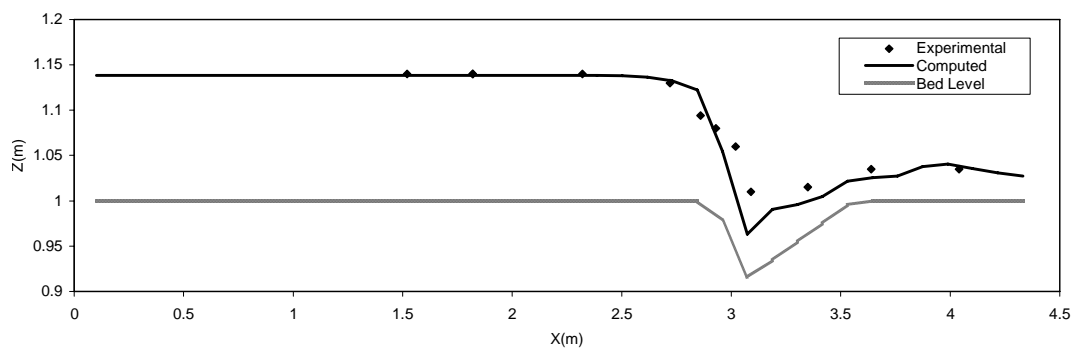


**Figure 4.** Comparison between model results and measurement data.

fluctuations at DIDAMAR Island, obtained from Admiralty Tide Table for the period of 12 days from December 2003 see Figure 6a, are imposed at HORMOZ Strait (the east end of the flow domain). The inflow from the Arvand River (located at the border line between IRAN and IRAQ centuries) is imposed at the end the estuary located at the north west of the flow domain. Considering the evaporations from the water surface and Coriolis effects, the flow patterns are formed due to the coasts and bed surface geometry and roughness.

In Figure 6b, the water surface elevation computed by the hydrodynamic model (thick line)

is compared with the predictions of the Admiralty Tide Table (thin line) at BUSHEHR Port which is located at the north part of the Persian Gulf. Since still water is consider at the start of the computations, there is a few days warm up period and then the results of the hydrodynamic model follow the Tide Table predictions. A few samples of numerical results which present computed water surface elevations and flow velocity are shown in Figure 7 (from the computations on the meshes with islands). Because of the mesh resolution, the flow simulation in the Persian Gulf island is considered in this study would take 10 times more

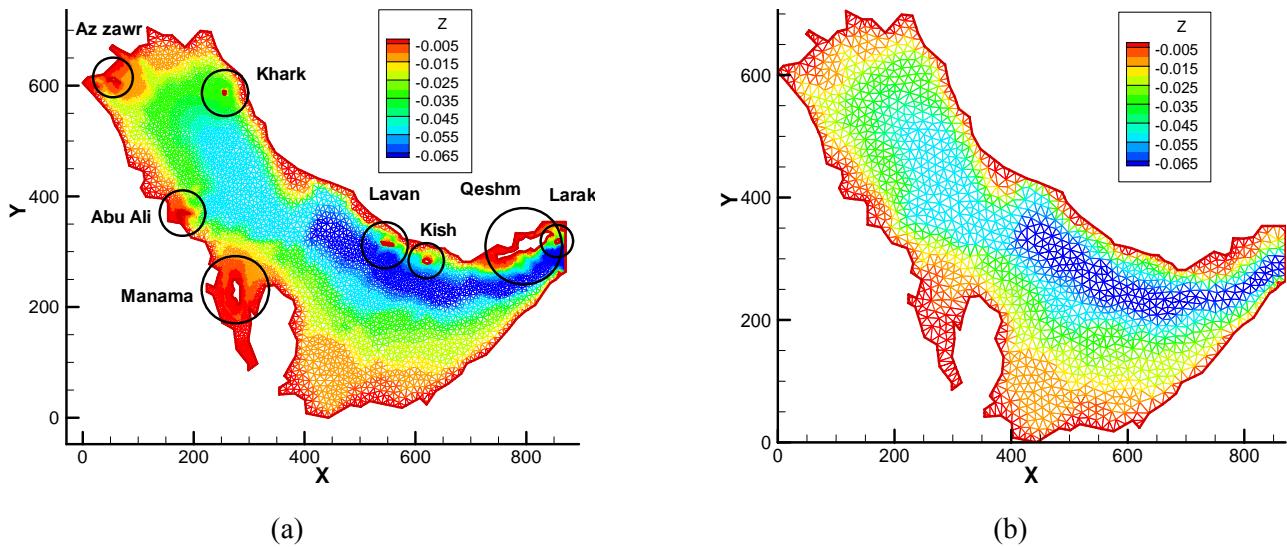


**Figure 5.** Two-dimensional discrete geometrical model; (a) considering major islands, (b) ignoring islands; Z is referred to the Persian Gulf bathymetry (km).

CPU-time than the case without the islands.

**6.2. Islands Effects** In this part, the effects of the islands are considered. Figure 8a and 8b shows the stream lines in the Persian Gulf, with and without islands.

In order to compare the obtained results of both simulation domains (with major islands and without islands), mean absolute percentage error (MAPE) was considered as a statistical performance evaluation. (Relation 8)

$$MAPE = \frac{1}{n} \sum_{i=1}^n \left| \frac{Q_i^I - Q_i^N}{Q_i^I} \right| \times 100 \quad (8)$$

Where n is the number of data,  $Q_i^I$  stands for the results computed with major islands of the model (surface water level and velocity), and  $Q_i^N$  is model results without the islands.

After investigation of model results on considering island, it can be concluded that considering islands would not affect the surface fluctuation even near islands, which shows an Average MAPE around 0.01 % next to the islands

and obviously far less than unity in other parts of the Persian Gulf.

But the story for velocities is completely different. Considering islands makes a considerable difference in computed velocities next to the islands. It worth's noting that from islands, the computed velocity values are similar for both cases. Table 1 presents an averaged amount of MAPE calculated within an arbitrary circular area around four major islands.

As can be seen in Table 1, islands in the solution domain will directly affect neighboring velocity patterns. The maximum difference in computed velocities can be observed near Qeshm Island. This might be due to its considerable size as well as considerable tidal fluctuations close to the HORMOZ Strait. Figure 9 depicts the differences between computed velocities at south of Qeshm Island (with approximately 1 km from the island).

## 7. CONCLUSIONS

A hydrodynamic model is developed for solving the depth averaged equations of continuity and motions on unstructured triangular mesh



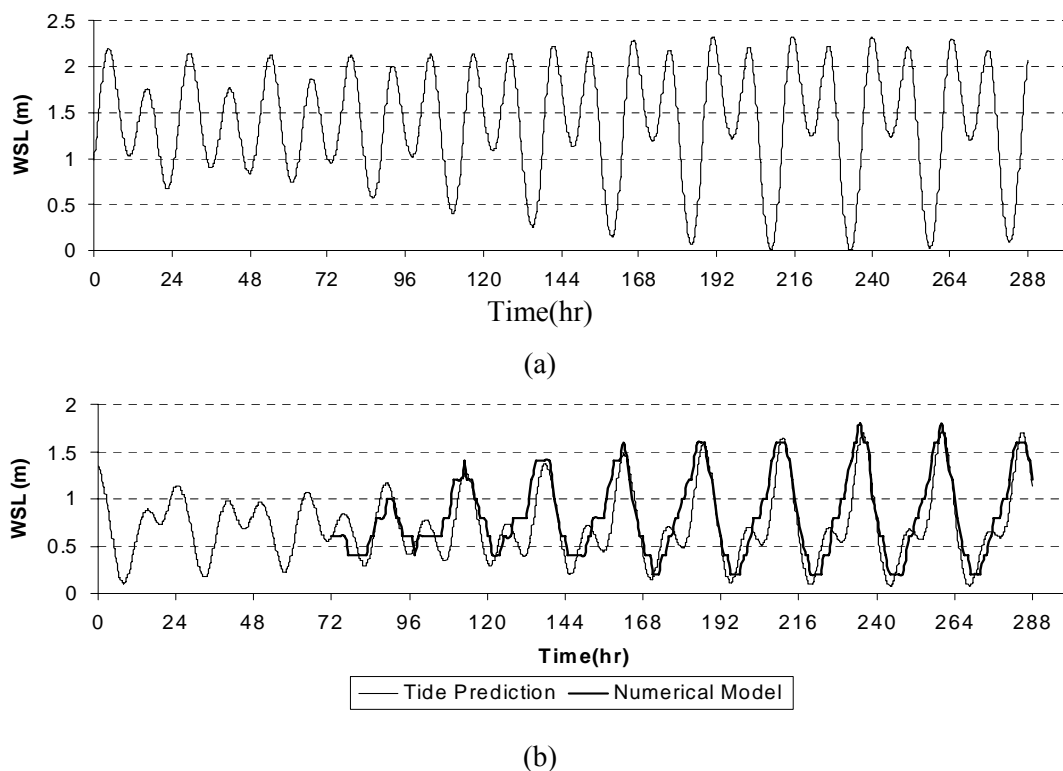


**Figure 6.** Water surface level fluctuations at: (a) HURMOZ strait, (b) BUSHEHR.

considering the bed elevation is successfully examined in this paper. The numerical results of fluctuating flow on flow domain with variable bed elevations presents acceptable agreements with the analytical solution. Considering tidal fluctuations at flow boundary, inflow from rivers, evaporations and Coriolis effects, bed surface geometry and roughness, the tidal flow patterns in Persian Gulf are successfully modeled. The results of the verification tests present accurate performance of the developed solve numerically solve the shallow water equations on geometrically complex flow field. The agreements between predictions of Admiralty Tide Table and flow patterns computed by hydrodynamic model are encouraging. The model was run in two different situations of considering and ignoring the major islands and an evaluation was done on the obtained results. The numerical investigations on computational modeling of tidal currents on the Persian Gulf shows that considering the islands will not produce considerable improvement in computed water surface fluctuations. The existence of the islands in

the computational mesh will provide different velocity results around islands. However, considering islands requires finer mesh and consequently gives rise to considerable computational work load.

## 8. ACKNOWLEDGEMENTS

The authors wish to thank K. N. Toosi University of Technology for supporting this research work and Mr. Ali Kermani (M. Sc. Graduate) for preparing geometric and analytical data as well as editing the paper.

## 9. REFERENCES

1. Lardner, R. W., Belen, M. S. and Cekirge, H. M., "Finite Difference Model for Tidal Flows in the Arabian Gulf", *Computational Mathematics with Applications*, Vol. 8, No. 6, (1982), 425-444.

2. Al-Rabeh, A. H., Gunay, N. and Cekrieger, H. M., "A Hydrodynamic Model for Wind-driven and Tidal Circulation in the Arabian Gulf", *Journal of Applied Mathematical Modeling*, Vol. 14, (1990), 410-419.
3. Evans-Roberts, D. J., "Tides in Persian Gulf", *Consulting Engineer*, Vol. 43, No. 6, (1979), 46-48.
4. Elahi, K. Z. and Ashrafi, R. A., "Tidal Modeling of Persian Gulf, in Hydraulic and Environmental Modeling: Coastal Waters", *International Conference on Computer Modeling of Seas and Coastal Regions and Boundary Elements and Fluid Dynamic*, Southampton, UK, (1992), 89-98.
5. Vreugdenhil, C. B., "Numerical Methods for Shallow Water Flow", Kluwer Academic Publisher, the Netherlands, (1994).
6. Castanedo, S., Medina, R. and Mendez, F. J., "Models for the Turbulent Diffusion Terms of Shallow Water Equations", *Journal of Hydraulic Engineering, ASCE*, Vol. 131, No. 3, (2005), 217-223.
7. Sabbagh-Yazdi, R. S. and Mohammad Zadeh Qomi, M.,

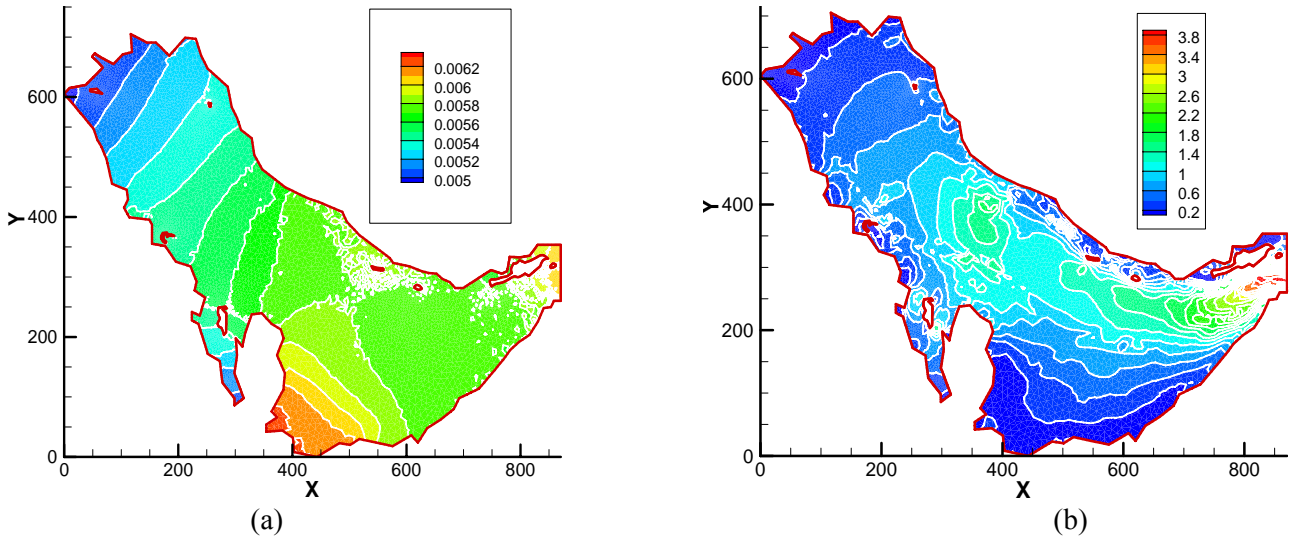


**Figure 7.** Computed results in an arbitrary time in terms of colour coded contour maps in two weeks tidal from 1/12/2003  
 (a): Water surface elevation (km) from mean sea level,  
 (b): Flow velocity (km/hr)).

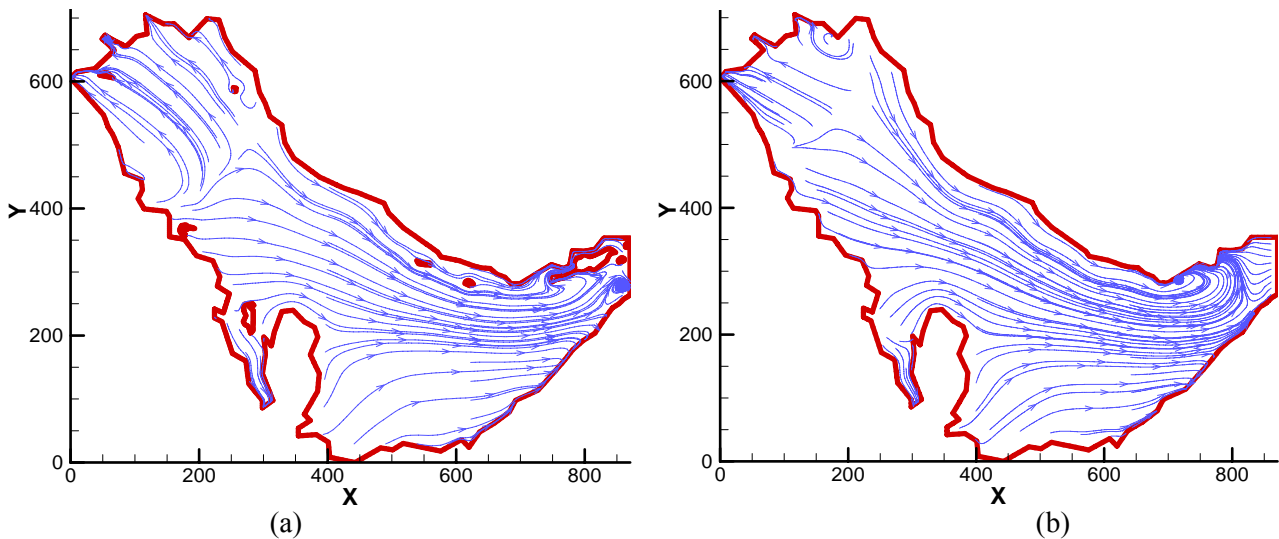


**Figure 8.** Typical computed stream traces in a certain time;  
 (a) with islands, (b) without islands.

**TABLE 1. Averaged MAPE of Velocity Around Islands,  
(From Two Computational Cases of Persian Gulf).**

Distance Island	Averged MAPE					
	1 Km	5 km	10 km	20 km	30 km	50 km
Kish	39 %	28 %	22 %	12 %	6 %	2 %
Khark	13 %	8 %	5 %	4 %	2 %	1 %
Qeshm	49 %	36 %	22 %	14 %	8 %	4 %
Manama	10 %	7 %	6 %	4 %	2 %	1 %

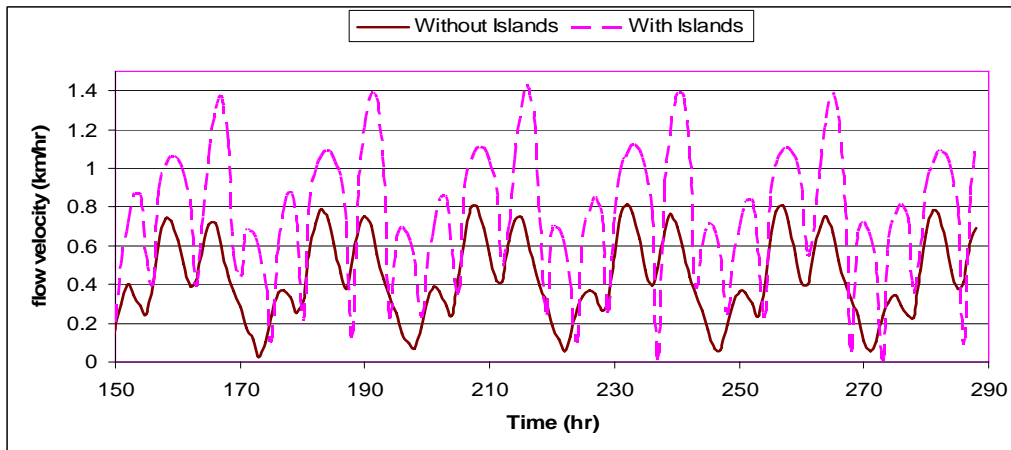


**Figure 9.** Model velocity results near Qeshm Island (second week of computation).

- “Finite Volume Solution of Two-Dimensional Convection Dominated Sub-Critical Flow Using Unstructured Triangular Meshes”, *International Journal of Civil Engineering*, Vol. 2, No. 3, (2004), 78-91.
8. Jameson, A., Schmidt, W. and Turkel, E., “Numerical Solution of the Euler Equations by Finite Volume Method using Runge Kutta Time Stepping Schemes”, *AIAA 14<sup>th</sup> Fluid and Plasma Dynamic Conference*, Paper No. 1259, Palo alto, California, (1981).
  9. British Admiralty, Admiralty Tide Tables, Hydrographic Department, Admiralty Charts and Publications, London, UK, Vol. 1, (1964).
  10. Report on Rainfall and surface currents in Iran, “Water Resource Management Organization of Iran (Farsi)”, Research Deputy, Tehran, (2003).
  11. Balzano, A., “Evaluation of Numerical Simulation of Wetting and Drying in Shallow Water Flow Models”, *Coastal Engineering*, Vol. 34, (1998), 83-107.
  12. Chen, C. L., “Analytical Solution for Tidal Model Testing”, *Journal of Hydraulic Engineering*, Vol. 115, No. 12, (1989), 1707-1714.
  13. Thompson, Joe F., Soni, Bharat K. and Weatherill, Nigel P., “Hand book of grid generation”, CRC Press, New York, USA, (1999).
  14. Ye, J. and McCorquodale, J. A., “Depth-Averaged Hydrodynamic Model in Curvilinear Collocated Grid”, *Journal of Hydraulic Engineering*, Vol. 123, No. 5,

(1997), 380-388.  
15. Zhou, Jian Guo, "Velocity-Depth Coupling in Shallow-

Water Flows", *Journal of Hydraulic Engineering*, Vol. 121, No. 10, (1995), 717-724.